

# Diversification and biodiversity dynamics of hot and cold spots

Carlos J. Melián<sup>1,\*</sup>, Ole Seehausen<sup>1</sup>,  
V́ctor M. Eguíluz<sup>2</sup>, Miguel A. Fortuna<sup>3</sup>, and Kristy Deiner<sup>4</sup>,

<sup>1</sup>Fish Ecology and Evolution Department,  
Center for Ecology, Evolution and Biogeochemistry,  
Swiss Federal Institute of Aquatic Science and Technology, Switzerland.

<sup>2</sup>Instituto de Física Interdisciplinar y Sistemas Complejos,  
Spanish Research Council, Universitat de les Illes Balears,  
Palma de Mallorca, Spain.

<sup>3</sup>Integrative Ecology Group  
Estación Biológica de Doñana (EBD-CSIC), Seville, Spain

<sup>4</sup>Department of Aquatic Ecology,  
Swiss Federal Institute of Aquatic Science and Technology, Switzerland.

Keywords: Metacommunity dynamics, landscape genetics, speciation theory,  
asymmetric gene flow, assortative mating, ecological drift.

Type of Article: Article

Number of figures: 2 (in color); Number of tables: 1

\* Corresponding author: Phone: +41 58 765 2208; Fax: +41 58765 2168;  
e-mail:carlos.melian@eawag.ch.

## 1 Abstract

2 The determinants that shape the distribution of diversity of life on Earth have been long dis-  
3 cussed and many mechanisms underlying its formation have been proposed. Yet connecting  
4 the biogeography of hot and cold spots of diversification and current biodiversity patterns to  
5 the microevolutionary processes remains largely unexplored. Here, we combine a landscape  
6 genetics model based on demographic stochasticity with a speciation model that can be inter-  
7 preted as a model of the evolution of premating incompatibility or assortative mating to map  
8 diversification rates in a spatial context. We show that landscape structure and the intensity  
9 and directionality of gene flow strongly influence the formation of hot and cold spots and its  
10 connection to patterns in species richness. Specifically, hot and cold spots form in landscapes  
11 in which gene flow is sufficiently strongly structured that the metacommunity nearly breaks up  
12 into several disconnected metacommunities. In such a landscape structure, speciation hot spots  
13 originate in the center or in the periphery of the landscape depending on whether the direction  
14 of net gene flow is from the periphery to the center or viceversa, respectively. However, for  
15 any given level of gene flow intensity, diversification rates are approximately twice higher in the  
16 center than in the periphery of the landscape. These results suggest that sinks may form diver-  
17 sification hot spots with higher probability than sources, in particular, those sinks surrounded  
18 by highly diversified sources in different locations of the landscape. Joining mechanistically  
19 microevolutionary and macroevolutionary processes on landscapes present many fascinating  
20 challenges and opportunities to connect the biogeography of diversification with biodiversity  
21 dynamics.

## 22 Introduction

23 Species richness varies strongly in geographical space (Gaston, 2000). The rates at which  
24 new species are produced and existing species go extinct too vary in space (Rabosky, 2009).  
25 Yet, it is still unclear how variation in speciation and extinction rates relates to variation  
26 in species richness although it has fascinated scientists since the birth of modern evolutionary  
27 biology (Wallace, 1855, 1876; Simpson, 1944; Dobzhansky, 1950). Species richness at any spatial  
28 scale reflects a balance between the tendency of lineages to form new species and species to  
29 go extinct (i.e., the diversification rate), and the variety of species that an environment can  
30 support (Rabosky, 2009). At a first glimpse, one might expect higher species richness where  
31 the net diversification rate is higher (i.e., a “hot” spot in terms of the number of speciation  
32 events, or a cradle of species diversity) but this is not necessarily so, because after their origin,  
33 species may change their distribution through range expansion and regional extinction, and  
34 speciation and extinction rates may vary independently of each other in space. Thus, diversity  
35 may accumulate in places with relatively low diversification rates, for instance in places with  
36 zero speciation and low extinction but high immigration (i.e., a diversification “cold” spot).  
37 Consequently, there is still considerable debate about how diversification relates in space to  
38 variation in species richness (Ricklefs, 2012; Mannion *et al.*, 2014).

39 By reconstructing phylogenetic trees of lineages of birds and mammals along a latitudinal  
40 gradient, a higher recent speciation rate but also higher recent extinction rates have been  
41 found at higher latitudes compared to the tropics (Weir & Schluter, 2007; Jetz *et al.*, 2012).  
42 These results are based on the average time since divergence of sister species, and intraspecific  
43 phylogroups and haplotypes, which tend to be shorter with much smaller variance in temperate  
44 regions than in tropical regions (but see (Tobias *et al.*, 2008)). Thus, these results suggest that  
45 the larger richness in the tropics in birds and mammals is due to lower extinction rates. In

46 a major review of the latitudinal species richness gradient, Mittelbach et al. (2007) come to  
47 the slightly different conclusion that current evidence points to the tropics as both a museum  
48 and a cradle, where taxa preferentially originate in the tropics and tend to also persist there  
49 longer (Mittelbach *et al.*, 2007). Consistent with this view, some studies have shown that  
50 the vast majority of bivalve lineages in the Sea had originated in the tropics, in spite of the  
51 strong sampling bias towards temperate zones (Jablonski *et al.*, 2006). Taken together these  
52 observations suggest that high latitudes have likely experienced more extinction and most in  
53 situ speciation events are recent, but rapid recent speciation is not uncommon in the tropics  
54 either (see also (Wagner *et al.*, 2014).)

55 Other studies found larger differences in diversification rates between Eastern and Western  
56 hemispheres than across latitudinal gradients (Jetz *et al.*, 2012). For instance, while cichlid fish,  
57 a group that diversifies predominantly in lakes, diversified faster in Africa than in the Neotropics  
58 (Genner *et al.*, 2007) mostly because of recent high speciation rates in African lakes, characins,  
59 another unusually species rich group of tropical freshwater fish is much more diversified in the  
60 extensive and geologically old river networks of the Neotropics and accumulated its diversity  
61 through low extinction rates without high speciation (Albert & Reis, 2011). Such observations  
62 suggest that the geographic and environmental structure of the landscape and its persistence  
63 through time play an important role in driving net diversification rate variation but that ef-  
64 fects may vary between lineages with different ecological characteristics. Additional evidence  
65 for the importance of the geographical structure of the landscape comes from investigations of  
66 the dynamics of the latitudinal diversity gradient through geological time using fossil records.  
67 Such studies have shown that the equatorial peak and poleward decline in species richness has  
68 not been a persistent pattern but it is restricted to the past 30 million years and a few earlier  
69 intervals (Mannion *et al.*, 2014) associated perhaps with the constellation of landmasses and

70 climate. Given the complexity of the empirically inferred relationships between diversification  
71 rates and diversity, but also the problems associated with inferring these relationships from  
72 incompletely sampled biotas and heterogeneous taxonomic knowledge, we suggest that theoret-  
73 ical modeling may be helpful to infer conditions under which relationships between variation  
74 in diversification rate and species richness in space are expected or not.

75 Several approaches have been developed to merge the geographic variation of diversifica-  
76 tion rates to landscape structure (Thompson, 2005; Lawson, 2013). Some have emphasized the  
77 connection between the microscopic analysis of ecological systems to the emergence of macroe-  
78 cological patterns (see for example, an island biogeography model developed by Gilpin and  
79 Diamond in the 70s (Gilpin & Diamond, 1976); a theory to connect abundance and distribu-  
80 tion patterns with diversification rates across a variety of taxa (Brown, 1984); a general model to  
81 connect, in addition to the structure of the landscape, landscape dynamics as a factor affecting  
82 species persistence (Keymer *et al.*, 2000); and how landscape complexity alter species diversi-  
83 fication and sorting in mammals (Vrba, 1992)). Yet, linking microevolutionary processes that  
84 generate reproductively isolated species to the macroecological patterns in species distributions  
85 and richness remain at an incipient stage mostly because of computational complexity.

86 In the present study, we investigate the connections between gene flow and landscape struc-  
87 ture with the spatial variation in diversification rates and species richness. We also study the  
88 emergence of hot and cold spots in speciation rates and how they relate to the distribution of  
89 species richness in the landscape. We define hot spots of diversification and species richness as  
90 geographic regions with high diversification rates or high species richness, respectively, while  
91 cold spots are geographic regions with low diversification rates or species richness. We ask,  
92 does the spatial structure of interconnected populations together with the intensity and direc-  
93 tionality of gene flow influence the formation of hot and cold spots in diversification and species

94 richness? If so, can we make predictions about the biogeography of hot and cold spots? In the  
95 present study we take a landscape genetics approach. We implement a neutral population ge-  
96 netic model for speciation to explore connections between spatial genetic population structure  
97 and gene flow directionality with the emerging dynamics of hot and cold spots in diversification  
98 and how these relate to spatial variation in species richness. Such an approach wants to make  
99 contributions to understanding of how macroecological patterns of species richness may emerge  
100 simply as a consequence of microevolutionary processes that act on individuals in populations  
101 causing them to diverge, speciate and go extinct in a persistent landscape, i.e., without the  
102 need to invoke changing landscapes through time.

103 Our results suggest that landscape structure and the intensity and directionality of gene  
104 flow strongly influence the formation of hot and cold spots of biological diversification and its  
105 connection to patterns in species richness. Specifically, hot and cold spots of diversification  
106 form in landscapes in which gene flow is sufficiently strongly structured that the metacommunity  
107 nearly breaks up into several disconnected metacommunities. Hot spots originate in the  
108 center or in the periphery of such landscapes depending on whether the direction of net gene  
109 flow is from the periphery to the center or viceversa, respectively. However, for any given level  
110 of gene flow intensity, diversification rates are approximately twice higher in the center when  
111 the direction of gene flow is to the center than in the periphery of the landscape when the di-  
112 rection of gene flow is away from the center. These results suggest that under the assumptions  
113 of our models, gene flow sinks may form diversification hot spots with higher probability than  
114 sources, in particular, those sinks surrounded by many sources. On the flip side of the coin,  
115 landscapes with symmetric gene flow of any intensity, landscapes with many isolated popula-  
116 tions or densely connected landscapes with asymmetric gene flow do not produce hot spots in  
117 our model. We discuss these results in the context of understanding the connection between

118 geographical variation in diversification and species richness patterns.

## 119 **The model**

120 Population genetics models of speciation and phenotypic models of speciation take into account,  
121 in most of the existing variations, three main processes: Migration dynamics, viability selection,  
122 and mating (Felsenstein, 1981; Kondrashov & Kondrashov, 1999; Dieckmann & Doebeli, 1999;  
123 Kirkpatrick & Ravigné, 2002; Van Doorn *et al.*, 2009). The order of these three processes and  
124 the complexity considered within each of these three components may have an effect on the  
125 dynamics of speciation (Felsenstein, 1981). In this study, we combine mutation, migration and  
126 drift with similarity-based mating in landscape genetics models to explore conditions under  
127 which hot and cold spots of diversification form in space. New species arise if a population  
128 becomes genetically too distant from its nearest relatives, species spread and go extinct through  
129 demographic stochasticity. In the following sections we introduce the landscape genetics models  
130 using random geometric landscapes and demographic stochasticity in three different gene flow  
131 scenarios, the speciation and extinction concepts used in this study and the method used to  
132 track diversification rate.

## 133 **Random geometric landscapes**

134 We consider landscapes consisting of randomly located sites (i.e., nodes with a spatial location  
135 given by  $x_i$  and  $y_i$ ) connected by dispersal events (i.e., links). This spatial network is embedded  
136 in an area of  $1000 \times 1000 \text{ km}^2$  (Figure 1) with a total number of sites,  $\mathcal{S}$ , equal to 1000. Two  
137 sites  $i$  and  $j$  are connected by dispersal events if the Euclidean distance between them,  $d_{ij}$ , is  
138 equal or smaller than a threshold distance,  $d_{max}$ . The largest fraction of connected sites, the  
139 giant component, depends on the distance threshold considered. We explored a range of values

140 for the distance threshold ( $20 \text{ km} < d_{max} < 100 \text{ km}$ ) that recovers the full range of sizes for  
 141 the giant component. That is, we explore landscape structure going from landscapes in which  
 142 all sites are completely disconnected to landscapes in which all sites are connected in a single  
 143 component (Figure 1) (Penrose, 2003).

## 144 Population dynamics and gene flow

145 At the beginning of the simulations in each replicate we have an initial population that spreads  
 146 instantaneously across the whole landscape. We assume that all sites are fully occupied and  
 147 have the same carrying capacity, i.e., population size at a given site  $i$ ,  $N_e^i$ , is equal to the site  
 148 environmental carrying capacity. The overall number of individuals at a given site is fixed, and  
 149 the total number of individuals in the landscape is  $N_e = N_e^1 + N_e^2 + N_e^3 + N_e^4, \dots, + N_e^S$ , with  
 150  $S$  the total number of sites.

151 The population evolves on the spatial network under a zero-sum birth and death process  
 152 in overlapping generations. This means that at each time step an individual dies from a  
 153 randomly chosen site  $i$ . This individual is replaced with a offspring coming from another  
 154 site (i.e., migrant) or from the same site than the death individual. Parents are chosen with  
 155 probability  $m$  from outside site  $i$  and with probability  $(1 - m)$  from the site  $i$ . To explore  
 156 the effect of the intensity (i.e., probability  $m$ ) and directionality (i.e., center to periphery  
 157 or viceversa) of gene flow on hot and cold spot formation we need to take into account the  
 158 spatial location of the parents coming to site  $i$ . We considered three models differing in the  
 159 directionality of gene flow: symmetric, centripetal and centrifugal gene flow (Brown, 1957;  
 160 Lemmon & Lemmon, 2008). In the symmetric model parents are chosen from the subset of  $j$   
 161 sites connected to the site  $i$  that satisfy the condition  $d_{ij} \leq d_{max}$ . In the centripetal gene flow  
 162 scenario, parents are chosen from the  $j$  sites connected to the site  $i$  that satisfy the condition



163  $d_{ij} \leq d_{max}$  as in the symmetric scenario, but now we only choose those  $j$  sites that are more  
 164 in the periphery than site  $i$ . Peripheral sites are those sites whose total sum of geographic  
 165 pairwise distance is equal or larger than for site  $i$ . In the centrifugal gene flow scenario, parents  
 166 are chosen from the  $j$  sites connected to the site  $i$  that satisfy the condition  $d_{ij} \leq d_{max}$  as in  
 167 the previous scenarios, but now we only choose those  $j$  sites that are more in the center than  
 168 site  $i$ . Center sites are those sites whose total sum of geographic pairwise distance is equal or  
 169 lower than for site  $i$ .

### 170 **Model 1: Symmetric gene flow**

In the simplest scenario for those  $i$  and  $j$  connected populations (i.e., geographic distance lower or equal than the radius,  $d_{ij} \leq d_{max}$ ), we consider gene flow of species  $k$  is only a function of the geographic distance between site  $i$  and  $j$ . Gene flow between site  $j$  and site  $i$  is

$$m_{ij} = \frac{m}{d_{ij}}, \quad (1)$$

171 where  $d_{ij}$  is the geographical distance between site  $i$  and  $j$ , and  $m$  determines the intensity of  
 172 gene flow.

### 173 **Model 2: Centripetal gene flow**

Under this scenario, gene flow from site  $j$  to site  $i$  depends not only on the distance between the two sites,  $d_{ij}$ , but parents are chosen preferentially from the periphery. Gene flow from site  $j$  to site  $i$  is

$$m_{ij} = \begin{cases} \frac{m}{d_{ij}} & \text{if } \sum_{k=1}^{\mathcal{S}} d_{ik} \leq \sum_{k=1}^{\mathcal{S}} d_{jk}, \\ 0 & \text{if } \sum_{k=1}^{\mathcal{S}} d_{ik} > \sum_{k=1}^{\mathcal{S}} d_{jk} \end{cases} \quad (2)$$

174 Formula (2) assumes that dispersal is directional from sites with higher total geographic distance  
 175 (where total geographic distance is defined as the sum over all distances between the focal site  
 176 and all other sites) to sites with a lower total geographic distance. If core sites are defined as

177 those that have lower total geographic distance than peripheral sites, then formula (2) implies  
 178 that **offspring** move from the periphery to the center of the landscape. (We remark there is no  
 179 net flow of individuals from the periphery to the center because the number of individuals in  
 180 each site remains constant.)

### 181 **Model 3: Centrifugal gene flow**

This is the opposite scenario than the above one: parents are now chosen preferentially from the center. Gene flow from site  $j$  to site  $i$  is

$$m_{ij} = \begin{cases} \frac{m}{d_{ij}} & \text{if } \sum_{k=1}^{\mathcal{S}} d_{ik} \geq \sum_{k=1}^{\mathcal{S}} d_{jk}, \\ 0 & \text{if } \sum_{k=1}^{\mathcal{S}} d_{ik} < \sum_{k=1}^{\mathcal{S}} d_{jk} \end{cases} \quad (3)$$

182 In this case, **offspring** move preferentially from the center to the periphery of the landscape.

### 183 **Species concept**

184 Each individual in our model contains a haploid genome consisting of an infinite string of  
 185 nucleotides. All genomes are identical at the outset and each offspring genotype is produced  
 186 from freely recombined parental haplotypes. This means there is no standing genetic variation  
 187 at the start of each run. The genetic similarity between two individuals  $k$  and  $l$ ,  $q_{kl}$ , is defined  
 188 as the proportion of identical nucleotides along the genome. The genetic similarity matrix,  $\mathcal{Q}$   
 189 =  $[q_{kl}]$ , contains all the pairwise similarity values,  $q_{kl}$ . In our models, this genetic similarity  
 190 matrix evolves as a consequence of mutation, mating and free recombination that produces a  
 191 haploid offspring that differs from both parents (Higgs & Derrida, 1992; Melián *et al.*, 2010).

192 We define a species as a group of individuals with the ability of interbreeding that are  
 193 reproductively isolated from other groups (Nei *et al.*, 1983). This means any two individuals  
 194 can mate and have fertile offspring if and only if their genetic similarity value is larger or equal  
 195 to the minimum value,  $q_{min}$ . Thus, for replacing a dead individual in site  $i$  parents  $k$  and  $l$  with

196 larger genetic similarity than the threshold,  $q_{kl} \geq q_{min}$ , are chosen with probability  $m$  from any  
 197 other  $j$  connected site,  $d_{ij} \leq d_{max}$ , and with probability  $(1 - m)$  from the site  $i$ . Mating pairs  
 198 that fulfill the condition  $q_{kl} \geq q_{min}$  have identical fitness, hence there is no selection on mating  
 199 compatibility in our model. Mating pairs that do not fulfill the condition  $q_{kl} \geq q_{min}$  do not  
 200 form, hence there is assortative mating determined by the genetic similarity threshold.

201 However, the ability of interbreeding does not imply that all conspecific individuals can  
 202 have fertile offspring between themselves. If we link every pair of individuals whose genetic  
 203 similarity is larger than the minimum value  $q_{min}$  (i.e., population graph), then two individuals  
 204 connected at least by one pathway through the population graph are considered conspecific,  
 205 even if the genetic similarity among them is smaller than  $q_{min}$ . Speciation occurs in our model  
 206 when all individuals with intermediate genotypes die. Values of  $q_{min}$  ranged from 0.93 to 0.96 in  
 207 our simulations. We note this definition of species and speciation through compatibility-based  
 208 assortative mating is not directly applicable to ecological speciation.

### 209 **Computing genetic similarity matrix to detect speciation events**

210 The genetic similarity matrix,  $\mathcal{Q} = [q_{kl}]$ , containing all the pairwise genetic similarity values,  
 211  $q_{kl}$ , has a size for the entire population of  $10^6 \times 10^6$  (1000 sites with 1000 individuals each).  
 212 This matrix is symmetric ( $q_{kl} = q_{lk}$ ). We store it as an adjacency list. The adjacency list  
 213 describes for each individual  $i$  the genetic similarity value with all individuals and the sites  
 214 where these individuals are. At each time step we update this adjacency list as a consequence  
 215 of changes in the genetic similarity values between the offspring and all the individuals in the  
 216 population following the method described in (Melián *et al.*, 2010). For each replicate, and  
 217 after 10000 generations (1 generation is 1000000 time steps) we start to count the components  
 218 each 10 generations following a depth-first search algorithm (Gabow, 2000). New speciation

219 events (i.e., components in the adjacency list) are then localized in space and the centroid of  
 220 the distribution of the new species calculated. This was done for 100000 generations for each  
 221 replicate and for a total of 100 replicates (see “Simulations” below). Computation time speed  
 222 up within each replicate with the number of generations because the adjacency list will be  
 223 decreasing in size due that some pairwise genetic similarity values  $q_{kl} < q_{min}$  (zero values in  
 224 the adjacency list.)

### 225 Spatial location of hot and cold spots

In order to compute the diversification rate, we track the spatial location of each speciation and extinction event. This information can be plotted after several speciation and extinction events and so we can map where the hot and cold spots in speciation and extinction events are. Speciation events occur when a population graph split into two or more distinct components (i.e., species). On the contrary, extinction events occur when a population graph disappears because the last individual has died. The spatial location of each speciation event was calculated as the mean geographic distance of all the sites  $N$  containing at least one individual that belong to the new species  $k$ . This center of gravity of sites containing the new species is given by

$$x = \frac{1}{N} \sum_{i=1}^N x_i \quad (4)$$

$$y = \frac{1}{N} \sum_{i=1}^N y_i \quad (5)$$

and the speciation rate for each spatial location is given by

$$\lambda_{x,y} = \frac{\#sp_{x,y}}{G}, \quad (6)$$

226 where  $G$  is the number of generations.

The site that harbored the last living individual of a given species is considered the spatial location of an extinction event. The extinction rate is then calculated as

$$\mu_{x,y} = \frac{\#ex_{x,y}}{G}, \quad (7)$$

and the diversification rate at a given spatial location,  $\Omega_{x,y}$ , can then be calculated as

$$\Omega_{x,y} = \lambda_{x,y} - \mu_{x,y}. \quad (8)$$

## 227 **Species richness**

228 Mapping each speciation and extinction event in the landscape allow us to track the number  
 229 of extant species. Thus, as for the diversification rate, we count the number of extant species  
 230 across generations for each replicate and plot this number as a function of the distance to the  
 231 center of the landscape.

## 232 **Simulations**

233 Our simulation is a stochastic, individual-based, zero-sum birth-death model linking gradual  
 234 genetic changes in populations with overlapping generations (microevolutionary processes) with  
 235 speciation events based on compatibility-based assortative mating driven by the genetic sim-  
 236 ilarity threshold (macroevolutionary processes). Specifically, we simulated the ecological and  
 237 evolutionary dynamics of populations of haploid individuals located at discrete sites randomly  
 238 distributed on a spatial network. Simulations were carried out with an initial population at  
 239 each site  $i$ ,  $N_e^i$ , of 1000 individuals for a total of 1000 sites. The population size and the number  
 240 of sites remained constant throughout the simulations.

241 Results for Figure 2 and 3 were obtained after 100 replicates and 100000 generations of a  
 242 single model run, where a generation is an update of the total number of individuals in the

243 landscape. Hot and cold spots plotted represent the mean values of 100000 slices ranging from  
 244 the center to the periphery of the network. We explored a broad range of landscapes using the  
 245 maximum distance to connect two sites and to determine the mating pool,  $20 \text{ km} < d_{max} < 100$   
 246 km. Population genetics parameter combinations explored: mutation rate,  $\mu \in (3 \times 10^{-4}, 10^{-5})$ ,  
 247 the intensity of gene flow,  $m \in (0.3, 0.001)$ , and the cut-off values to count speciation events and  
 248 species richness in the transient and equilibrium dynamics represented as the minimum genetic  
 249 similarity value to define a species,  $q_{min} \in (0.96, 0.93)$ . **Total number of species reached a**  
 250 **mean value after approximately 75000-90000 generations (variation due to the different initial**  
 251 **parameter values). At that stage, speciation rate equals extinction rate and all hot spots**  
 252 **disappear.**

## 253 Results

254 In order to connect the dynamics of speciation hot and cold spots formation to biodiversity  
 255 patterns, we first generate a range of landscapes, from completely connected (Figure 1A repre-  
 256 sents a landscape with sites  $i$  and  $j$  connected if  $d_{ij} \leq d_{max} = 75\text{km}$ ) to completely disconnected  
 257 sites (Figure 1C,  $d_{max} = 25\text{km}$ ). Between these two landscape structures we have a clustered  
 258 landscape with groups of interconnected sites (Figure 1B,  $d_{max} = 50\text{km}$ ).

259 Diversification hot spots are possible only when the spatial network is near the percolation  
 260 threshold. This means hot spot formation occurred in landscapes that were nearly broken up  
 261 into several disconnected metacommunities and only with centripetal or centrifugal gene flow.  
 262 **Figure 1B can illustrate the idea of a metacommunity as several sites sparsely connected across**  
 263 **the whole spatial network. Thus, each aggregation of sparsely connected sites can be defined**  
 264 **as a metacommunity.** Centripetal gene flow model produces higher diversification rate in the  
 265 center than in the periphery of the landscape (Figure 2A, dotted red line with gene flow,  $m$

266 = [0.1, 0.3]). Centrifugal gene flow model produces higher diversification rate in the periphery  
 267 than in the center of the landscape (Figure 2A, continuous red line with gene flow,  $m = [0.1,$   
 268  $0.3]$ ). Diversification rate decreases with low gene flow in both scenarios (Figure 2A, dotted  
 269 and solid black line with gene flow,  $m < 0.1$ .)

270 How do speciation and extinction rate and how do diversification rate and species richness  
 271 correspond in the landscape? We found speciation and extinction rate spatially corresponding  
 272 in the landscape (Figure 2B, centripetal, and 2C, centrifugal). Extinction rate peaks in the hot  
 273 spots of diversification but it does not increase as much as the speciation rate (Figure 2B and  
 274 2C). Approximately twice higher extinction rates were observed where the hot spots formed in  
 275 the centripetal gene flow model (compare blue line in Figure 2B for the centripetal with the  
 276 Figure 2C for the centrifugal gene flow model). Diversification rate and species richness do also  
 277 spatially correspond in the landscape (Figure 3). The centripetal gene flow model produced  
 278 hot spots and high species richness in the center (Figure 2A-B and 3). The centrifugal gene  
 279 flow model produced hot spots and high species richness in the periphery (Figure 2A-C and 3).  
 280 Centripetal gene flow predicts approximately twice higher speciation rate, diversification rate  
 281 and species richness compared to the centrifugal gene flow model (Figure 2A, diversification  
 282 rate approx. 0.004 vs. 0.002 and Figure 3, species richness 150 vs. 65). Centripetal gene flow  
 283 model also produced higher  $\gamma$ -species richness than the centrifugal gene flow model,  $206 \pm 49$   
 284 vs.  $94 \pm 35$ .

285 In summary, our predictions suggest there is an “asymmetry” in the intensity of the hot  
 286 spots formation. Centripetal gene flow model consistently predicted higher speciation and  
 287 extinction rate, diversification rate and species richness than the centrifugal gene flow model  
 288 (Figure 2 and 3). This “asymmetry” in the intensity of the hot spot formation has consequences  
 289 for biodiversity: the number of species accumulating in the center is consistently higher than

290 in the periphery. This result indicates that those sectors of the network receiving migrants  
291 (i.e., sinks) may form diversification hot spots, and thus acquire higher species richness, than  
292 those areas in the network delivering migrants (i.e., sources). This seems particularly true in  
293 those sinks close to the center of the species distributions that are surrounded by many sources  
294 connected to highly differentiated areas in the landscape.

## 295 Discussion

296 Our study adds to previous attempts to connect microevolutionary dynamics and macroevolu-  
297 tionary patterns in a mechanistic framework (Gavrilets, 2004; Gavrilets & Vose, 2007; de Aguiar  
298 *et al.*, 2009; Kopp, 2010; Melián *et al.*, 2010; Rosindell & Phillimore, 2011; Davies *et al.*, 2011).  
299 Our goal was to understand patterns in the geography of the hot and cold spots in diversification  
300 rate and their connection to geographical variation in species richness. Our analysis showed  
301 that the origin of speciation hot and cold spots required directional gene flow in landscapes  
302 connected to an extent that they nearly broke up into several disconnected metacommunities  
303 (Figure 1B). Centripetal gene flow dynamics with net gene flow from the periphery to the center  
304 generated higher diversification rates in the hot spots compared to the centrifugal gene flow  
305 model in which net gene flow is from the center to the periphery (Figure 2). Our results showed  
306 that the formation of speciation hot spots was inhibited in densely connected landscapes, as  
307 well as in landscapes with most communities isolated and in landscapes with symmetric gene  
308 flow patterns regardless of the degree of isolation. Our results also suggest that speciation and  
309 extinction rate variation (Figure 2B and 2C) together with diversification rate variation (Figure  
310 2A) and standing amounts of species richness (Figure 3) have correspondence in the landscape.

311 In the following we discuss our model results in the context of island biogeography theory and  
312 macroecological species richness gradients. Previous studies suggest that the geographic and



313 environmental structure of the landscape and its persistence through time play an important  
314 role in driving net diversification rate variation (Ricklefs, 2012; Mannion *et al.*, 2014). Island  
315 biogeography theory with speciation has been applied to two very different island scenarios:  
316 oceanic islands and lakes. Whereas oceanic islands and island archipelagoes tend to be strongly  
317 isolated from the nearest mainland with gene flow restricted to rare colonization events, large  
318 lakes are often connected to one or several rivers and receive continued gene flow from the rivers.  
319 Our models suggest that the geometry of the island network combined with the directionality  
320 of gene flow strongly determine whether and where hot spots in diversification and in the  
321 corresponding species richness arise. For example, our models predict lower speciation rates  
322 when islands are in the periphery of the network of habitat patches than when islands are central  
323 to such networks. Our results indicate that diversification hotspots do not form when islands  
324 are disconnected from the source sites (i.e., isolated with low gene flow), whereas our models  
325 predict hot spots of diversification in islands that are connected to the sources by moderate  
326 levels of gene flow. By analogy this may predict larger rates of diversification and larger species  
327 richness in continental lakes that are connected to several streams providing colonists and  
328 continued gene flow, than in oceanic islands that are in the periphery of the network of habitat  
329 islands. More generally these results suggest that the landscape structure combined with the  
330 directionality of gene flow may play a critical role in determining whether and where a radiation  
331 zone or a hot spot of diversification arises (Gillespie *et al.*, 2008; Rosindell & Phillimore, 2011).

332 How do hot and cold spot formation relate to sources and sinks and species richness? Our  
333 results suggest that hot spots occurred with higher probability in those fractions of the network  
334 receiving migrants from a highly diversified set of sources and that these sinks also accumulated  
335 higher species richness than the areas in the network that delivered migrants (i.e., the sources).  
336 This suggests distinct geographic patterns in the relationship between species richness and the

337 diversification rate may arise (Figure 2 and 3) in the absence of spatial variation in carrying ca-  
338 pacities across the landscape. Extending these models by explicitly modeling sources and sinks  
339 with differential growth rates (or carrying capacities) and productivity across the landscape  
340 may show even more distinct geographic patterns of diversification rate and species richness.  
341 Recent investigations of the fossil record have shown that the tropical peak and poleward de-  
342 cline in species richness has not been a persistent pattern throughout the Phanerozoic, but is  
343 restricted to intervals of the Palaeozoic and the past 30 million years (Mannion *et al.*, 2014).  
344 Our models can also be extended to incorporate climatic regimes and landscape dynamics to  
345 provide a dynamic system in which to explore spatiotemporal diversity fluctuations. These  
346 extended models can tell us how much complexity is required to make predictions that match  
347 periods of peaks or flattened species richness gradients as observed in the fossil record.

348 We contrasted biodiversity dynamics in models with completely symmetric (Fig. 2A blue  
349 line) versus completely asymmetric (Fig. 2A red lines) migration and gene flow. Asymmetric  
350 migration patterns are common in nature. Dendritic river networks, inclusive of lakes embedded  
351 into them, are a classical example where migration and gene flow in the downstream direction  
352 tends to be much stronger than in the opposite direction. Dispersal in the Sea is another classical  
353 example where ocean currents determine the dominant direction (Bonfil *et al.*, 2005), and rare  
354 long distance dispersal of birds across oceans may often be predictable by the predominant  
355 direction of winds (Thorup *et al.*, 2007). **The detection of speciation events in space using**  
356 **very similar models have shown that location of speciation in a symmetric migration model**  
357 **strongly depends on the level of genetic variation (Gavrilets *et al.*, 2000).** In the future, our  
358 modeling framework should be extended to situations that combine symmetric and asymmetric  
359 gene flow to explore the dependency of the emergence of diversification hotspots on the extent  
360 of deviation from symmetry and genetic variation. In our study, we contrasted dynamics with

361 migration rates of approx. 0.1 (Fig. 2A black lines) with those when migration rates were  
362 larger than 0.1 but smaller than 0.3 (Fig. 2A red lines). Another interesting extension would  
363 be to simulate a larger range of gene flow values and investigate the shape of the relationship  
364 between migration rate, landscape structure and the intensity of diversification hotspots.

365 How do the availability of space or resources and the strength and direction of selection  
366 change the results presented in this study about the hot and cold spot formation? Diversification  
367 may depend, at least in part, on the availability of space and resources, landscape structure  
368 and gene flow among populations, the architecture of the genotypes and the strength and  
369 form of selection (Gavrilets & Losos, 2009). Our approach did not explicitly test for sources  
370 and sinks because we assumed equal growth rates across the landscape, nor did we assume  
371 any asymmetry in competition or trophic interactions as possible mechanisms for structuring  
372 diversity in our landscapes, hence a neutral theory of biodiversity was applied. Our approach  
373 instead takes into account assortative mating, landscape structure and the directionality of gene  
374 flow as the main drivers of speciation events across the landscape (Welch, 2004). Our models  
375 cannot capture the microevolutionary dynamics associated with ecological speciation fueled by  
376 adaptations to niches (Rundle & Nosil, 2005), or speciation driven by sexual selection (Maan  
377 & Seehausen, 2011). **Specifically, we have considered infinite genomes with all genes having a**  
378 **weak effect on divergence. It would be interesting to contrast our results from results assuming**  
379 **finite genomes with a small number of genes having a strong effect, where speciation would**  
380 **also involve isolation by distance.** Extending the models introduced in this study, by explicitly  
381 considering habitat, sexual selection **or finite genomes** may alter the geography of hot and cold  
382 spots presented in new and unexpected ways. Nonetheless the models explored here may be  
383 useful as a benchmark to compare their predictions in the geographic variation of hot and cold  
384 spots of diversification to biologically more realistic scenarios.

## 385 Acknowledgments

386 We thank Alejandro Rozenfeld and Rebecca Best for valuable suggestions which greatly im-  
387 proved the manuscript. CJM was supported by the Swiss National Science Foundation project  
388 31003A-144162. MAF was supported by a postdoctoral fellowship (JAE-Doc) from the Program  
389 “Junta para la Ampliacion de Estudios” co-funded by the Fondo Social Europeo.

## 390 References

- 391 de Aguiar, M.A.M., Baranger, M., Baptestini, E.M., Kaufman, L. & Bar-Yam, Y. (2009).  
392 Global patterns of speciation and diversity. *Nature*, 460, 384–387.
- 393 Albert, J.S. & Reis, E.R. (2011). *Historical Biogeography of neotropical freshwater fishes*. Uni-  
394 versity of California Press. Berkeley, USA.
- 395 Bonfil, R., Meýer, M., C., S.M., Johnson, R., O’Brien, S., Oosthuizen, H., Swanson, S., Kotze,  
396 D. & Paterson, M. (2005). Transoceanic migration, spatial dynamics, and population linkages  
397 of white sharks. *Science*, 310, 100–103.
- 398 Brown, J.H. (1984). On the relationship between abundance and distribution of species. *The*  
399 *American Naturalist*, 124, 255–279.
- 400 Brown, W.L. (1957). Centrifugal speciation. *Quarterly Review of Biology*, 32, 247–277.
- 401 Davies, J.T., Allen, D.P., Borda de Água, L., Regetz, J. & Melián, C.J. (2011). Neutral  
402 biodiversity theory can explain the imbalance of phylogenetic trees but not the tempo of  
403 their diversification. *Evolution*, 65, 1841–1850.
- 404 Dieckmann, U. & Doebeli, M. (1999). On the origin of species by sympatric speciation. *Nature*,  
405 400, 354–357.
- 406 Dobzhansky, T. (1950). Evolution in the tropics. *American Scientists*, 38, 209–221.
- 407 Felsenstein, J. (1981). Skepticism towards santa rosalia, or why are there so few kinds of  
408 animals? *Evolution*, 35, 124–138.
- 409 Gabow, H.N. (2000). Path-based depth-first search for strong and biconnected components.  
410 *Information Processing Letter*, 74, 107–114.

- 411 Gaston, K.J. (2000). Global patterns in biodiversity. *Nature*, 405, 220–227.
- 412 Gavrilets, S. (2004). *Fitness Landscapes and the Origin of Species*. (Princeton University Press,  
413 Princeton).
- 414 Gavrilets, S., Li, H. & Vose, M.D. (2000). Patterns of parapatric speciation. *Evolution*, 54,  
415 1126–1134.
- 416 Gavrilets, S. & Losos, J.B. (2009). Adaptive radiation: Contrasting theory with data. *Science*,  
417 323, 732–737.
- 418 Gavrilets, S. & Vose, A. (2007). Case studies and mathematical models of ecological speciation.  
419 2. palms on an oceanic island. *Molecular Ecology*, 16, 2910–2921.
- 420 Genner, M.J., Seehausen, O., Lunt, D.H., Joyce, D.A., Shaw, P.W., Carvalho, G.R. & Turner,  
421 G.F. (2007). Age of cichlids: New dates for ancient lake fish radiations. *Mol. Biol. Evol.*, 24,  
422 1269–1282.
- 423 Gillespie, R., Claridge, E.M. & Goodacre, S. (2008). Biogeography of French Polynesia: Diver-  
424 sification within and between a series of hotspot archipelagoes. *Phil. Trans. Roy. Soc. Lond.*,  
425 363, 3335–3346.
- 426 Gilpin, M.E. & Diamond, J.M. (1976). Calculation of immigration and extinction curves from  
427 the species-area-distance relation. *Proceedings of the National Academy of the Sciences of*  
428 *the USA*, 73, 4130–4134.
- 429 Higgs, P.G. & Derrida, B. (1992). Genetic distance and species formation in evolving popula-  
430 tions. *Journal of Molecular Evolution*, 35, 454–465.

- 431 Jablonski, D., Roy, K. & Valentine, J.W. (2006). Out of the tropics: Evolutionary dynamics of  
432 the latitudinal diversity gradient. *Science*, 314, 102–106.
- 433 Jetz, W., Thomas, G.H., Joy, J.B., Hartmann, K. & Mooers, A.O. (2012). The global diversity  
434 of birds in space and time. *Nature*, 491, 444–448.
- 435 Keymer, J.E., Marquet, P.A., Velasco-Hernández, J.X. & Levin, S.A. (2000). Extinction thresh-  
436 olds and metapopulation persistence in dynamic landscapes. *The American Naturalist*, 156,  
437 478–494.
- 438 Kirkpatrick, M. & Ravigné, V. (2002). Speciation by natural and sexual selection: models and  
439 experiments. *The American Naturalist*, 159, S22–S35.
- 440 Kondrashov, A.S. & Kondrashov, F.A. (1999). Interactions among quantitative traits in the  
441 course of sympatric speciation. *Nature*, 400, 351–354.
- 442 Kopp, M. (2010). Speciation and the neutral theory of biodiversity. *Bioessays*, 32, 564–570.
- 443 Lawson, L.P. (2013). Diversification in a biodiversity hot spot: landscape correlates of phylo-  
444 geographic patterns in the african spotted reed frog. *Molecular Ecology*, 22, 1947–1960.
- 445 Lemmon, A.R. & Lemmon, E.M. (2008). A likelihood framework for estimating phylogeographic  
446 history on a continuous landscape. *Syst. Biol.*, 57, 544–561.
- 447 Maan, M.E. & Seehausen, O. (2011). Ecology, sexual selection and speciation. *Ecology Letters*,  
448 14, 591–602.
- 449 Mannion, P.D., Upchurch, P., Benson, R.B.J. & Goswami, A. (2014). The lati-  
450 tudinal biodiversity gradient through deep time. *Trends in Ecology and Evolution*  
451 (<http://dx.doi.org/10.1016/j.tree.2013.09.012>).

- 452 Melián, C.J., Alonso, D., Vázquez, D.P., Regetz, J. & Allesina, S. (2010). Frequency-dependent  
453 selection predicts patterns of radiations and biodiversity. *PLoS Comput Biol*, 6, e1000892.
- 454 Mittelbach, G.G., Schemske, D.W., Cornell, H.V., Allen, A.P., Brown, J.M., Bush, M.B., Har-  
455 rison, S.P., Hurlbert, A.H., Knowlton, N., Lessios, H.A., McCain, C.M., McCune, A.R.,  
456 McDade, L.A., McPeck, M.A., Near, T.J., Price, T.D., Ricklefs, R.E., Roy, K., Sax, D.V.,  
457 Schluter, D., Sobel, J.M. & Turelli, M. (2007). Evolution and the latitudinal diversity gradi-  
458 ent: speciation, extinction and biogeography. *Ecology Letters*, 10, 315–331.
- 459 Nei, M., Maruyama, T. & Wu, C.I. (1983). Models of evolution of reproductive isolation.  
460 *Genetics*, 103, 557–579.
- 461 Penrose, M.D. (2003). *Random Geometric Graphs*. Oxford Univ. Press, Oxford, UK.
- 462 Rabosky, D.L. (2009). Ecological limits and diversification: alternative paradigms to explain  
463 the variation in species richness among clades and regions. *Ecology Letters*, 12, 735–743.
- 464 Ricklefs, R.E. (2012). Disconnects in diversity. comment on "the global diversity of birds in  
465 space and time". *Nature*, 491, 1–2.
- 466 Rosindell, J. & Phillimore, A.B. (2011). A unified model of island biogeography sheds light on  
467 the zone of radiation. *Ecology Letters*, 14, 552–560.
- 468 Rundle, H. & Nosil, P. (2005). Ecological speciation. *Ecology Letters*, 8, 336–352.
- 469 Simpson, G.G. (1944). *Tempo and mode in evolution*. Columbia Univ. Press, New York.
- 470 Thompson, J.N. (2005). *The Geographic Mosaic of Coevolution*. (University of Chicago Press,  
471 Chicago).



- 472 Thorup, K., Bisson, I.A., Bowlin, M.S., Holland, R.A., Wingfield, J.C., Ramenofsky, M. &  
473 Wikelski, M. (2007). Evidence for a navigational map stretching across the continental u.s.  
474 in a migratory songbird. *Proceedings of the National Academy of Sciences of the U. S. A.*,  
475 104, 18115–18119.
- 476 Tobias, J.A., Bates, J.M., Hackett, S. & Seddon, N. (2008). Comment on “the latitudinal  
477 gradient in recent speciation and extinction rates of birds and mammals”. *Science*, 319,  
478 901c.
- 479 Van Doorn, G.S., Edelaar, P. & Weissing, F.J. (2009). On the origin of species by natural and  
480 sexual selection. *Science*, 326, 1704–1707.
- 481 Vrba, E.S. (1992). Mammals as a key to evolutionary theory. *Journal of Mammalogy*, 73, 1–28.
- 482 Wagner, C.E., Harmon, L.J. & Seehausen, O. (2014). Cichlid species-area relationships are  
483 shaped by adaptive radiations that scale with area. *Ecology Letters*.
- 484 Wallace, A.R. (1855). On the law which has regulated the introduction of new species. *Annals*  
485 *and Magazine of Natural History*, 16, 184.
- 486 Wallace, A.R. (1876). *The Geographical Distribution of Animals: with a study of the relations*  
487 *of living and extinct faunas as elucidating the past changes of the Earth’s surface*. Macmillan  
488 Co. London, UK.
- 489 Weir, J.T. & Schluter, D. (2007). The latitudinal gradient in recent speciation and extinction  
490 rates of birds and mammals. *Science*, 315, 1574–1576.
- 491 Welch, J.J. (2004). Accumulating Dobzhansky-Muller incompatibilities: Reconciling theory  
492 and data. *Evolution*, 58, 1145–1156.

## 493 Figure caption

494 **Figure 1. Random geometric landscapes as geographic template for population**  
 495 **dynamics.** By using a distance threshold  $d_{max}$  to connect 1000 randomly located sites across a  
 496 landscape of  $1000 \times 1000 \text{ km}^2$ , we obtained spatial networks with different levels of connectivity.  
 497 Three of them are shown here and also an speciation event in **B. A)**, Depicts a densely connected  
 498 network generated using  $d_{max} = 75 \text{ km}$ . **B)**, A spatial network near the percolation threshold  
 499 ( $d_{max} = 50 \text{ km}$ ). The percolation threshold is a connectivity level (given by a minimum  
 500 threshold distance  $d_{max}$ ) beyond which all sites that are connected in a single component,  
 501 called giant component, start to organizing into many smaller disconnected components. In **B**  
 502 we zoom out an speciation event. The individual with the largest node size dies forming a new  
 503 “red” species within the site. An speciation event could also occur from an individual dying  
 504 outside the focal site. **C** , Depicts a fragmented network generated using  $d_{max} = 25 \text{ km}$ .

505 **Figure 2. Diversification hot and cold spots. A)**, Diversification rate ( $\Omega$ , y-axis) as a  
 506 function of the distance to the center (x-axis) of a  $1000 \times 1000 \text{ km}^2$  landscape. Centripetal  
 507 gene flow model produces higher diversification rate in the center than in the periphery of  
 508 the landscape (dotted red line represents the mean values after sampling the intensity of gene  
 509 flow,  $m$ , from a uniform distribution with range  $\mathcal{U}[0.1, 0.3]$ , see inset). Centrifugal gene flow  
 510 model produces higher diversification rate in the periphery than in the center of the landscape  
 511 (continuous red line represents the mean values after sampling the intensity of gene flow,  $m$ ,  
 512 from a uniform distribution with range  $\mathcal{U}[0.1, 0.3]$ , see inset). Diversification rate decreases  
 513 with low gene flow in both scenarios (dotted and solid black line with gene flow,  $m < 0.1$ .) The  
 514 maximum distance used in those plots to connect two sites and to determine the mating pool  
 515 was  $35\text{km} < d_{max} < 55\text{km}$ . Symmetric gene flow model with all sites isolated does not produce  
 516 hot spots (Blue line and landscape in **E** show the results for a maximum distance to connect

517 two sites and to determine the mating pool between,  $d_{max} < 25\text{km.}$ ) **B**), Speciation ( $\lambda$ , red line,  
 518 y-axis) and extinction ( $\mu$ , blue line, y-axis) rate for the centripetal gene flow model with gene  
 519 flow,  $m = [0.1, 0.3]$ . Diversification hot spot is produced in the center of the landscape (**D**).  
 520 **C**), Speciation ( $\lambda$ , red line, y-axis) and extinction ( $\mu$ , blue line, y-axis) rate for the centrifugal  
 521 gene flow model with gene flow,  $m = \mathcal{U}[0.1, 0.3]$ . Diversification hot spot is produced in the  
 522 periphery of the landscape (**F**). Plotted lines represent the mean values of  $10^5$  sections ranging  
 523 from the center to the periphery of the network.

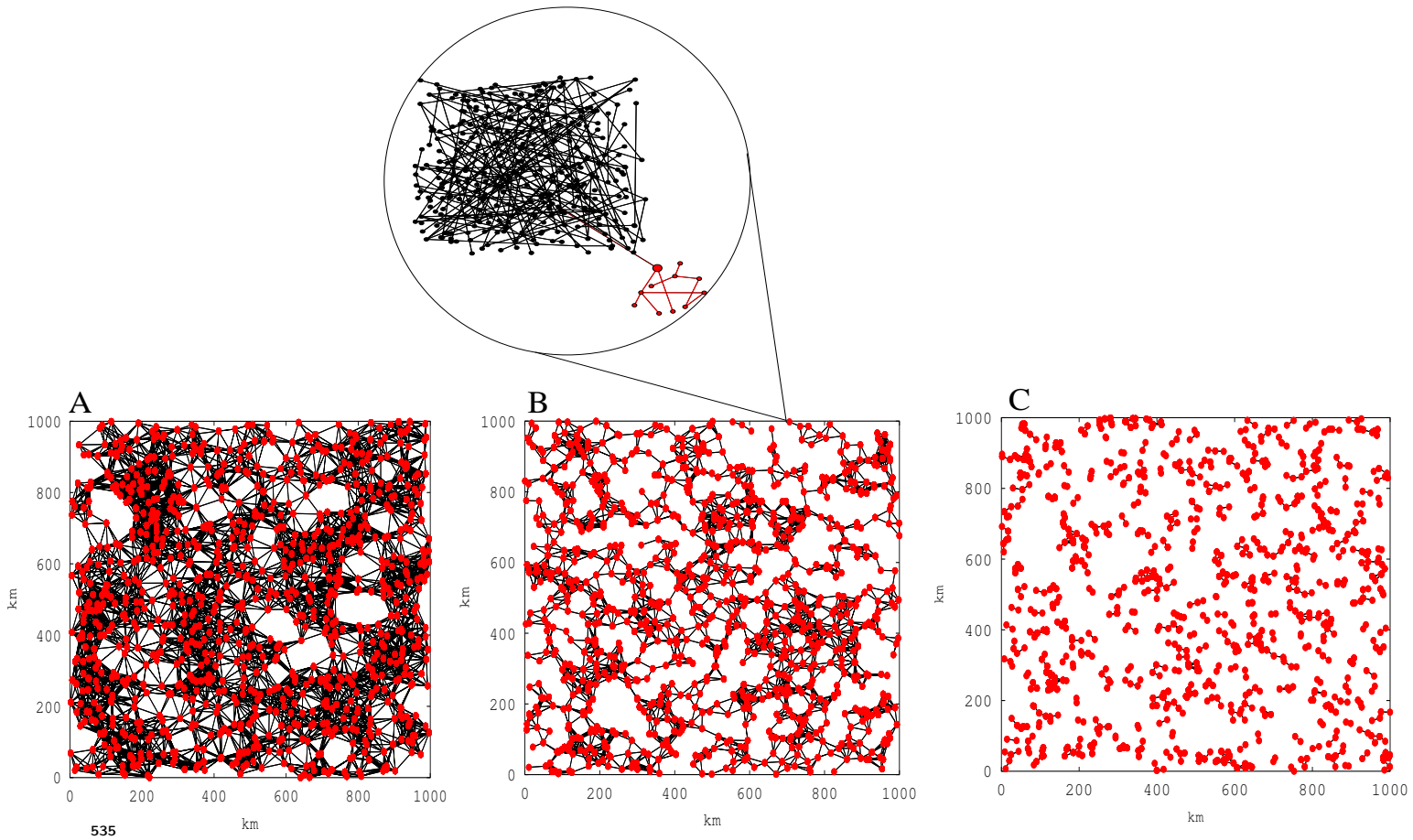
524 **Figure 3. Species richness in hot and cold spots.** Species richness as a function of its  
 525 distance to the center of a  $1000 \times 1000 \text{ km}^2$  landscape. The centripetal gene flow model produces  
 526 higher richness (dotted black line, represents the mean values after sampling the intensity of  
 527 gene flow,  $m$ , from a uniform distribution with range  $\mathcal{U}[0.1, 0.3]$ ) than the centrifugal gene flow  
 528 scenario (continuous line, represents the mean values after sampling the intensity of gene flow,  
 529  $m$ , from a uniform distribution with range  $\mathcal{U}[0.1, 0.3]$ ). Diversification rate and species richness  
 530 have correspondence in the landscape (compare Figure 2A with 3). Plotted lines represent the  
 531 mean values of  $10^5$  slices ranging from the center to the periphery of the network.

532 **Tables**

Table 1		<b>Glossary of mathematical notation</b>
<b>Notation</b>	<b>Definition</b>	
$\mathcal{S}$	Total number of sites	
$N_e^i$	Number of individuals in site $i$	
$N_e$	Total number of individuals in the landscape	
$(x_i, y_i)$	Spatial location of site $i$	
$d_{ij}$	Euclidean geographical distance between site $i$ and $j$	
$\mathcal{D}$	Geographic distance matrix containing all pairwise distances, $d_{ij}$	
$d_{max}$	Maximum geographic distance to connect two sites	
$q_{kl}$	Genetic similarity between individual $k$ and $l$	
$\mathcal{Q}$	Genetic similarity matrix containing all the pairwise similarity values, $q_{kl}$	
$m$	Intensity of gene flow	
$m_{ij}^k$	Gene flow from site $j$ to site $i$ for species $k$	
$q_{min}$	Minimum genetic similarity to have fertile offspring	
$\mu$	Mutation rate per nucleotide per birth-death cycle	
$\lambda_{x,y}$	Speciation rate in spatial location $(x, y)$	
$\mu_{x,y}$	Extinction rate in spatial location $(x, y)$	
$\Omega_{x,y}$	Diversification rate in spatial location $(x, y)$	

533

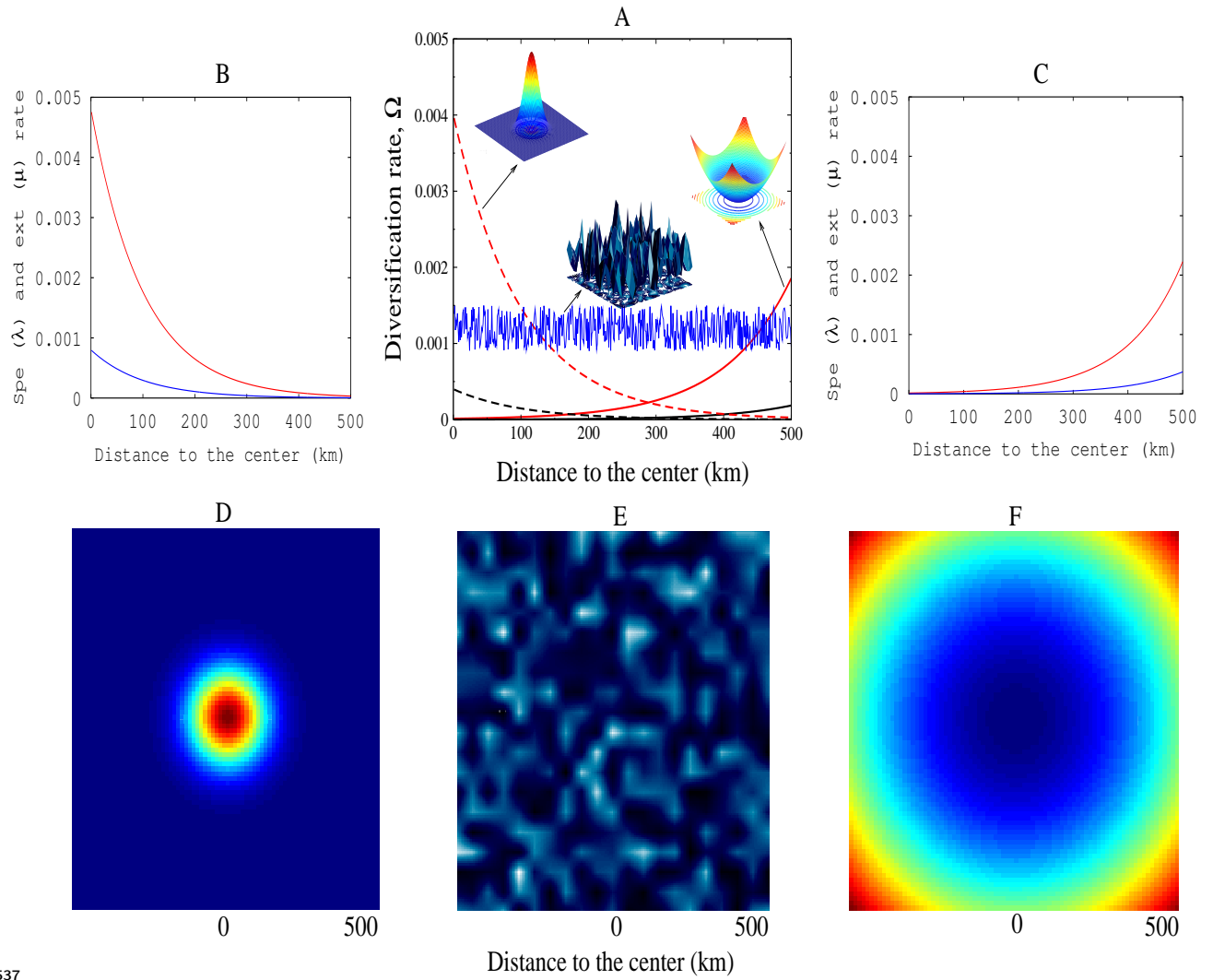
534 **Figures**



535

536

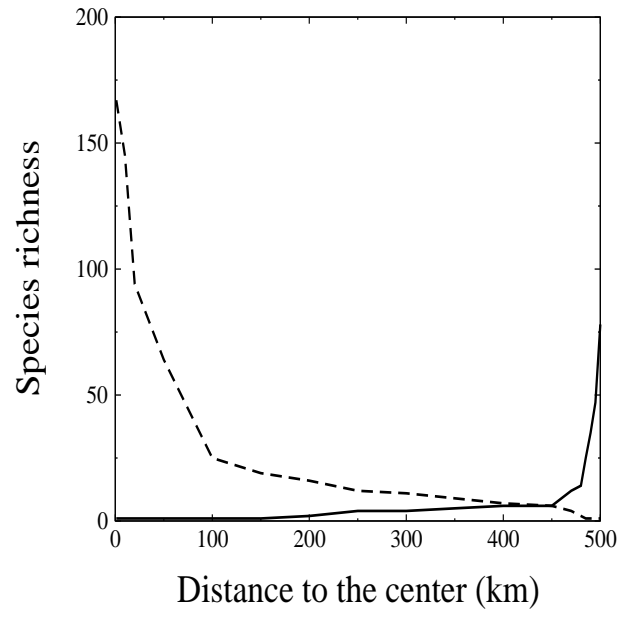
Figure 1



537

538

Figure 2



539

540

Figure 3